J Solid State Electrochem (2009) 13:679–685
DOI 10.1007/s10008-008-0601-8

ORIGINAL PAPER

Time-derivative cyclic voltabsorptometry for voltammetric characterization of catechin film on a carbon-paste electrode: one voltammogram becomes four

Jian-Bo He · Yuan Zhou · Fan-Shun Meng

Received: 15 April 2008 / Accepted: 22 May 2008 / Published online: 14 June 2008

Abstract Using (+)-catechin electrodeposited on a carbon-paste electrode as a model system, we have demonstrated the usefulness of the time-derivative cyclic voltabsorptometry for voltammetric characterization of the deposited films, in the case when not only the deposited species but also the same ones in free solution participated in redox processes. A long-optical-path thin-layer cell was used for the voltabsorptometric measurements. The potential-dependent absorption signals were monitored for catechin at 252 and 279 nm in B-R buffer electrolytes with pH=1.8. The combination of voltabsorptometry with voltammetry enabled one measured cyclic voltammogram to become four, which were attributed to catechin and its oxidized state, in free solution or in deposited state, respectively. The surface coverage of the electrode was evaluated from the cyclic voltammograms obtained for the deposited catechin, which decreased with the increasing scan rate. Also, the deposited species was found to make a major contribution to the total voltammetric current, especially at higher scan rates.

Keywords Deposited film · Cyclic voltabsorptometry · Cyclic voltammetry · UV-Vis spectroelectrochemistry · Catechin

Introduction

It is very common that the electroactive organic/biological molecules are chemically bonded to electrode surfaces under appropriate conditions of electrolysis. The widespread interest in the redox-deposited films has been demonstrated by their applicability in the area of chemically modified electrodes [1–4]. Multicycle cyclic voltammetry has been widely used for the preparation of the surface-immobilized films, usually based on the preadsorption of the immobilized molecules on electrode surfaces [2–4]. In general cases, both the preadsorbed species and the same species in free solution, are more or less involved in redox processes. Therefore, the charges of the redox peaks in the cyclic voltammogram (CV) include the contributions of the species in both states and cannot be directly used for the evaluation of the surface coverage. The objective of this work is to obtain CVs of the adsorbed species by subtracting the contributions of the species in free solution from the measured CV.

The combination of voltammetry and spectrophotometry offers the possibility of recording simultaneously CV and cyclic voltabsorptomogram (CVA) [5–10]. This method can separately monitor the specific absorbing species involved in the electrode process via setting the corresponding characteristic absorption wavelengths. The time-derivative cyclic voltabsorptomogram (DCVA), with a shape similar to that of the corresponding CV, usually has the voltabsorptometric peaks better defined than the respective voltammetric peaks [5, 9] due to the advantage of background free data collection. In recent years, more attention has been paid to cyclic voltabsorptometry, which was used mostly to investigate the redox processes within conducting polymer films [6–8] or protein films [9, 10] on indium-tin oxide optical transparent electrodes. In this work, the CVA measurements were conducted in a long-optical-path thin-layer spectroelectrochemical cell (SE-cell), which allowed an opaque working electrode to be used and the species in the thin-layer chamber to be

J.-B. He (✉) · Y. Zhou · F.-S. Meng
Anhui Key Laboratory of Controllable Chemical Reaction & Material Chemical Engineering,
School of Chemical Engineering, Hefei University of Technology,
Hefei 230009 Anhui Province, People's Republic of China
e-mail: jbhe@hfut.edu.cn

monitored, by a light transmission mode parallel to the electrode surface. In this case, the DCVA data stood for the potential-dependent reaction rates of the species in solution near the electrode surface (not involving the same species deposited on the electrode surface) and was presently used to produce the CVs of the species in free solution.

Catechin (CA) has been used as an electrode modifier by Salimi et al. [1] for the amperometric detection of dopamine in the presence of ascorbic acid. Zare and Habibirad [2] recently reported that a very stable electroactive film of CA was electrochemically deposited on the surface of activated glassy carbon electrode for the electrocatalytic oxidation of hydrazine. Based on these reports, we used (+)-CA electrodeposited on carbon-paste electrode as a model system in this work. As an important natural antioxidant, CA has attracted particular attention because of its efficient free-radical scavenging activity [11, 12]. Electrochemical methodologies have been widely used for CA in the studies of oxidation mechanism [11, 13], electroanalysis [14], metal-chelating [15], anti/pro-oxidant effects [16, 17], CA-modified electrodes [1, 2], etc. In aqueous media, CA showed at least three anodic voltammetric peaks, corresponding to the successive oxidations of hydroxyl groups at different positions [13]. In the relevant literatures [14–18], the first voltammetric peak of CA was unambiguously attributed to the oxidation of the catechol 3′,4′-dihydroxyl groups on the B-ring (Fig. 1). Papers dealing with quantitation of the antioxidant activity of many phenolic compounds were focused mainly on the first voltammetric peak [16–18] because the exceptionally high contribution to the antioxidative properties can be attributed to the catecholic structural unit of these molecules [16]. In this work, the multicycle potential scan was performed in the potential range of the first redox couple for the surface-immobilization of CA since the further oxidation in the higher potentials may produce nonelectroactive products blocking the electrode surface [13]. On the other hand, the oxidation pathway of CA at physiological pH (7.4) was complicated by the subsequent dimerization reactions, in which the 3′,4′-quinone intermediate, as a powerful electrophile, suffered attack by a CA unit leading to dimeric products [19, 20]. Therefore, the deposition of CA should be carried out in acidic media, just as an optimum pH value of 1.5 was selected by Zare and Habibirad for attaching CA to the surface of the glass carbon (GC) electrode [2].

Experimental

Reagents

(+)-CA is reagent-grade materials from Fluka (Tokyo, Japan). Spectrograde graphite powder (320 meshes, Shanghai Chemical Works, Shanghai, China) was used for the construction of the graphite-wax (GW, 5:2 w/w) working electrode. Doubly-distilled water from an all-glass distillatory apparatus was used. High pure N_2 was used for solution deaeration. All other chemicals were of analytical grade from Shanghai Chemical Works.

The 0.2 M Britton–Robinson buffered solutions plus 0.5 M KCl were prepared as the supporting electrolytes with various pH values. With the aid of ultrasonication, 1.0 mM stock solution of CA was prepared with ethanol and stored at 4 °C in a refrigerator. Before being used, it was diluted to various convenient concentrations by mixing with buffer-supporting electrolyte.

Apparatus

Ultraviolet-visible (UV-Vis) absorption spectra and chronoabsorptometric data were measured using a model UV-2500 spectrophotometer with UV probe data software (Shimadzu, Kyoto, Japan). Electrochemical measurements were carried out on a model CHI 660 microcomputer-based electrochemical analyzer (CHENHUA, Shanghai, China).

A three-electrode system was used, which consisted of a GW working electrode, a platinum grid counter electrode, and a $Ag/AgCl/KCl_{sat}$ reference electrode. The GW electrode was selected since its surface is easily renewed and presents a low background current and a wide range of working potentials. A disk GW electrode with a smaller geometrical area of 8 mm^2 was used for the common CV experiments, while a quadratic one with a larger area of 80 mm^2 was used for the in situ spectroelectrochemical

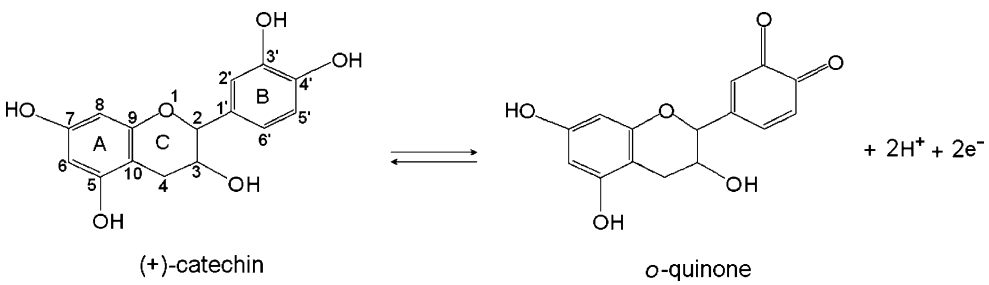

Fig. 1 Schematic of the redox reaction of (+)-CA

measurements. The long-optical-path thin-layer SE-cell was a commercially available, 10-mm quartz photometric cell, in which the three-electrode system was assembled [21]. The length of the optical path and the thickness and volume of the thin layer were 10 mm, 0.2 mm, and 16 μL, respectively. The time constant of the SE-cell was less than 1 ms in 0.5 M KCl solution, which was characterized by chronoamperometric experiments.

Procedure

Before the experiment, the electrolytic cell was washed with water and ethanol successively for 1 min under ultrasonication. All the experiments were carried out at room temperature (22±1 °C). CA solutions were bubbled with N_2 for about 15 min to remove dissolved oxygen before being put into the cell. The GW electrode was degreased with ethanol for 3 min and then washed with water before each measurement.

For the spectroelectrochemical experiment, a 1.0-ml portion of CA solution was injected into the SE-cell through the thin-layer chamber and then infiltrated into the two side chambers, ensuring no gas bubbles formed in the thin-layer compartment. The in situ UV-Vis absorption spectra were measured while the thin-layer solution was electrolyzed under potentiostatic conditions. Kinetic absorbance monitoring coupled with CV scans was taken at certain wavelengths to follow the concentration changes of species in the thin-layer solution. A preaccumulation step was always performed at the initial potential of 0.15 V for an accumulation time of 60 s in this work.

Results and discussion

Cyclic voltammetry

The CVs of CA were recorded in a conventional cell with the disk GW working electrode, as shown in Fig. 2. A couple of well-shaped CV peaks P_a/P_c appeared corresponding to the redox of the 3′,4′-dihydroxyl moiety at the B-ring (catechol moiety) of CA [13, 16]. The oxidation reaction led to the formation of CA 3′,4′-quinone (abbreviated to CAQ), as shown in Fig. 1. The peak potentials of both P_a and P_c were dependent linearly on the pH of solution, $E_{pa}/V = 0.603 - 0.055\text{pH}(R = -0.995)$ and $E_{pc}/V = 0.557 - 0.053\text{pH}(R = -0.996)$, respectively, both slopes supporting a reaction mechanism involving an equal number of electrons and protons. At the same time, the currents of both the peaks decreased obviously with the increase of pH. In the following investigations, a pH value of 1.8 was selected for the surface-immobilization of CA, as explained in the "Introduction."

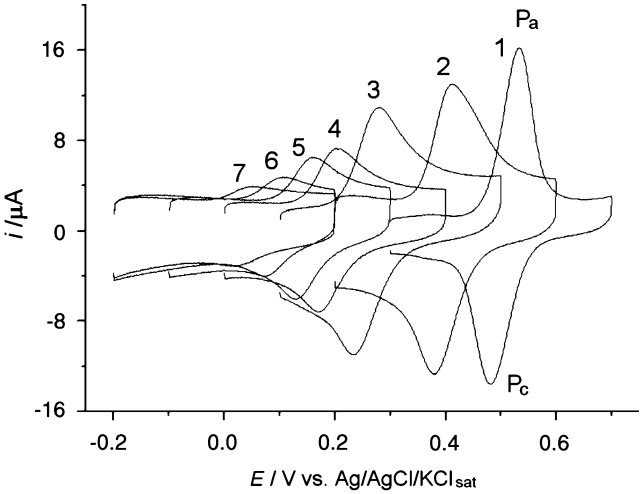

Fig. 2 CVs of 50 μM CA recorded at scan rate 100 mV s^{-1}. pH=1.8 (*1*), 3.3 (*2*), 5.7 (*3*), 7.0 (*4*); 8.0 (*5*), 9.2 (*6*), 10.4 (*7*)

The influence of potential scan rate on the CV peaks has been investigated in the range of 10–500 mV s^{-1} (Fig. 3). At the slower scan rate of 10 mV s^{-1}, the peak potential separation (ΔE_p) of the CV couple was as small as 11 mV. Such a small ΔE_p in a bulk CV experiment suggested a couple of quasireversible adsorption waves [22]. With the increase of scan rate up to 500 mV s^{-1}, the ΔE_p was increased up to about 120 mV, due to the increasing contributions of both electron transfer polarization and ohmic potential drop. On the other hand, the anodic peak current (after background correction) was observed to be nearly proportional to the

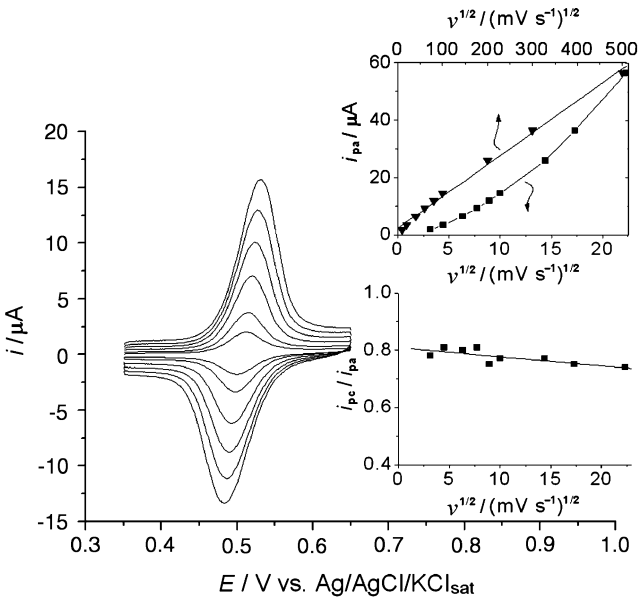

Fig. 3 CVs of 50 μM CA (pH=1.8) recorded at different scan rates: 10, 20, 40, 60, 80, and 100 mV s^{-1}. *Insets*: Scan rate dependencies of the peak current i_{pa} (*upper*) and the peak current ratio i_{pc}/i_{pa} (*lower*)

scan rate v (but not $v^{1/2}$) (the upper inset), as predicted theoretically for a surface diffusionless electrochemistry.

As is well known, the formed 3′,4′-quinones are generally quite reactive and can be attacked by a variety of nucleophiles, leading to Michael-type coupling products. The mechanism has been thought to consist of a fast electron transfer followed by an irreversible coupling of the two radicals or by an irreversible phenolate-phenoxyl radical coupling [11]. For an electron transfer process coupled with irreversible following chemical transition, the backward/forward peak current ratio i_{pc}/i_{pa} is expected to increase with increasing scan rate. However, the very slight decrease of i_{pc}/i_{pa} with scan rate was observed in the solution of pH=1.8 containing 50 μM CA, as is shown in Fig. 3 (the lower inset), which was consistent with the earlier reports—in acidic solutions at low concentrations, the coupling reactions were significantly suppressed and 3′,4′-quinone was the most abundant oxidation product [20]. Therefore, polymerization and electrode-inactivation effects were thereby almost completely avoided under our conditions. This is very important for the deposition of CA film with electrochemical activity.

Dynamic UV-Vis spectrum under constant potential

The UV-Vis spectrum change of CA (0.1 mM, pH=1.8) was measured in the SE-cell at the potential of 0.6 V to monitor the first oxidation of CA. Before electrolysis, CA exhibited its characteristic absorption band at 279 nm (the first line in Fig. 4, band I). After the potential was applied at 0.6 V, the absorption band I decreased to some extent while the absorption around 252 nm (band II) increased obviously, giving two isosbestic points at 272 and 290 nm, respectively. Similar spectral change had been observed also during the autoxidation of epigallocatechin gallate under aerobic conditions, leading to the formation of 3′,4′-quinonoid structure via semiquinone radical intermediate [23]. The seeming background change of the spectra in Fig. 4 was due to the formation of another wide and low absorption band centered at 386 nm.

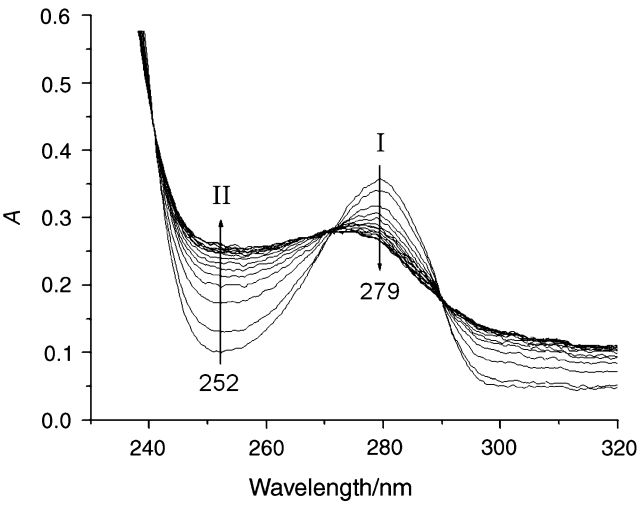

Fig. 4 Spectrum change during the oxidation of 0.1 mM CA (pH=1.8) at potential of 0.60 V. Spectral tracing was repeated every 60 s after the potential was applied. The *first line* was recorded before electrolysis

As shown in Fig. 4, the spectral change of the thin-layer solution indicates that not only the CA preadsorbed on electrode surface but also that in free solution was involved in the redox reaction. In the following investigations, the absorbances at the two bands (A_{279} and A_{252}) were monitored to follow the changes of the concentrations of CA and CAQ in the thin-layer solution during the cyclic potential scans, to estimate the contribution of the species in free solution to the total voltammetric currents.

Thin-layer cyclic voltabsorptometry

The CVA signals at the wavelengths 279 and 252 nm were monitored during the multicycle CV scan between 0.15 and 0.65 V in the SE-cell containing 0.1 mM CA (pH=1.8). The results obtained under the condition of slow scan of 2 mV s^{-1} are shown in Fig. 5a and b. The absorbances at both wavelengths changed periodically (Fig. 5b) with the alternate appearance of the redox voltammetric peaks (Fig. 5a). In the potential range of peak P_a, the absorbance A_{279} decreased, whereas A_{252} increased, indicating the decrease of CA and the increase of its product in the thin-layer solution due to the oxidation of CA. At the peak P_c, the contrary changes in absorbances occurred due to the reduction of CAQ.

The DCVAs, as shown in Fig. 5c, were obtained by differentiating the CVA data in Fig. 5b. A couple of differentiated peaks were presented in both the DCVAs, corresponding to the CV peaks P_a and P_c, respectively. Because of the superposition of the absorption bands of CA and CAQ, the DCVA data would be resolved in order to distinguish the contributions from each species in solution. For this resolution, the molar absorptivities (ε) of CA and CAQ at the two wavelengths were measured in the same medium as in Fig. 5. The obtained results show that $\varepsilon_{279,CA}= 3.52\times 10^3 cm^{-1} M^{-1}$, $\varepsilon_{279,CAQ} = 2.49 \times 10^3 cm^{-1}M^{-1}$, $\varepsilon_{252,CA} = 0.60 \times 10^3 cm^{-1}M^{-1}$, $\varepsilon_{252,CAQ} = 2.31 \times 10^3 cm^{-1}M^{-1}$, respectively. Further discussion is given below.

Four CVs derived from DCVA data

It is clear that both species deposited on the electrode surface and those in free solution were involved in the reactions of peaks P_a and P_c,

$$\begin{matrix} CA_{dep} \\ CA_{sol} \end{matrix} \underset{P_c}{\overset{P_a}{\rightleftharpoons}} \begin{matrix} CAQ_{dep} \\ CAQ_{sol} \end{matrix} + 2H^+ + 2e^-. \quad (1)$$

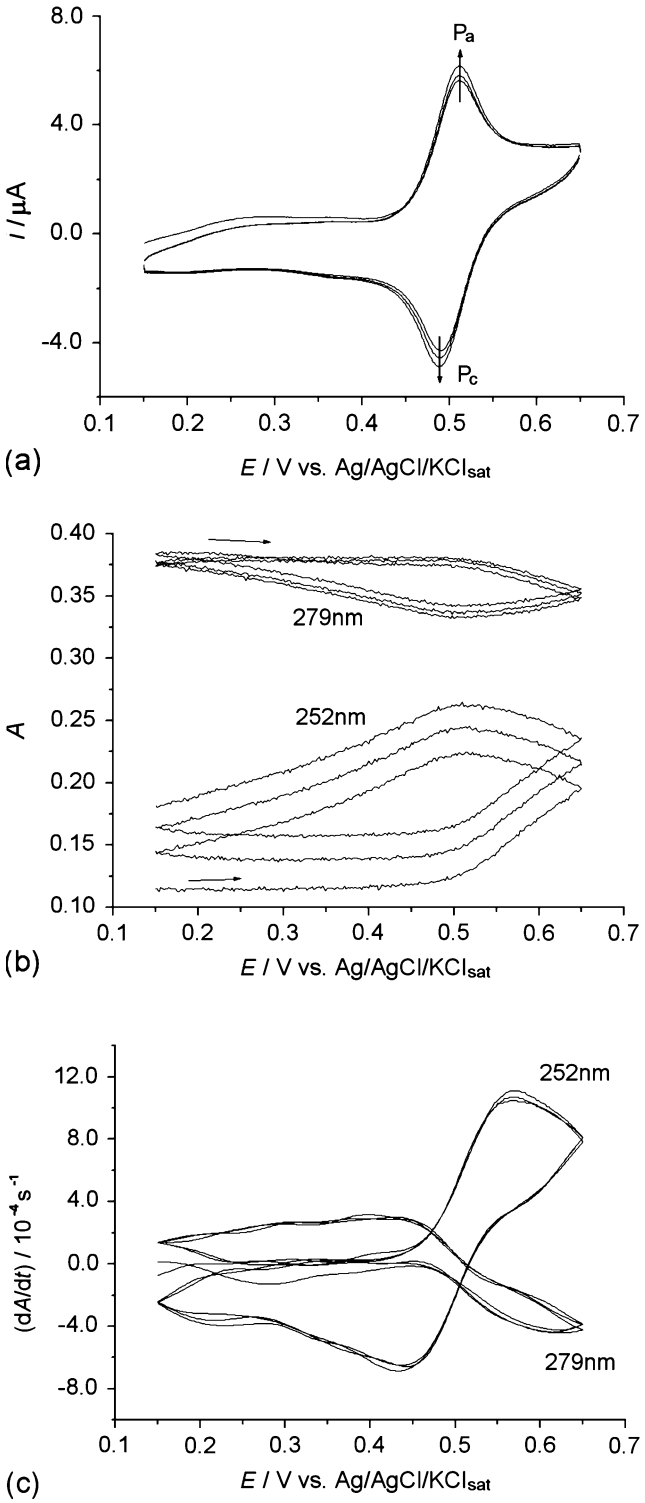

Fig. 5 Multicycle CV (**a**), CVAs (**b**), and DCVAs (**c**) of 0.1 mM CA (pH=1.8). Scan rate, 2 mV s^{-1}; cycle number, 3; wavelength, 279 and 252 nm

Because both CA and CAQ in thin-layer solution contributed to the absorptions at two bands (see Fig. 4), according to the Lambert–Beer's law, the time-derivative absorbances for the wavelengths of 252 and 279 nm can be expressed by the following equations:

$$\frac{dA_{252}}{dt} = \varepsilon_{252,CA} l \frac{dc(CA_{sol})}{dt} + \varepsilon_{252,CAQ} l \frac{dc(CAQ_{sol})}{dt} \quad (2)$$

$$\frac{dA_{279}}{dt} = \varepsilon_{279,CA} l \frac{dc(CA_{sol})}{dt} + \varepsilon_{279,CAQ} l \frac{dc(CAQ_{sol})}{dt} \quad (3)$$

from which we can obtain the reaction rate equations of CA and CAQ in free solution:

$$-\frac{dc(CA_{sol})}{dt} = \frac{\varepsilon_{252,CAQ}}{l\Sigma}\frac{dA_{279}}{dt} - \frac{\varepsilon_{279,CAQ}}{l\Sigma}\frac{dA_{252}}{dt} \quad (4)$$

$$\frac{dc(CAQ_{sol})}{dt} = \frac{\varepsilon_{252,CA}}{l\Sigma}\frac{dA_{279}}{dt} - \frac{\varepsilon_{279,CAQ}}{l\Sigma}\frac{dA_{252}}{dt} \quad (5)$$

where l is the optical path length (10 mm), $\sum = \varepsilon_{279,CAQ}\varepsilon_{252,CA} - \varepsilon_{279,CA}\varepsilon_{252,CAQ}$, and other parameters have their usual meanings.

Both reaction rates in Eqs. 4 and 5 can also be expressed in terms of current, according to the Faraday's law, $i=nFV(\pm dc/dt)$, where n is the number of electrons transferred (n= 2), V is the volume of the thin-layer chamber (16 μL), and F is the Faraday constant. Based on Eqs. 4 and 5, we can reconstruct the CV plots, $i(CA_{sol})$ vs $E(t)$ and $i(CAQ_{sol})$ vs $E(t)$, from the DCVA data (dA_λ/dt vs $E(t), \lambda = 279, 252\text{nm}$) (for this task, a simple computer program was prepared). Figure 6a shows two CVs calculated from the concentration changes of CA and CAQ in free solution, respectively. The difference in current between these two CVs, that is, $-dc(CA_{sol})/dt \neq dc(CAQ_{sol}/dt)$, can be due to the transition between the dissolved and the deposited species (see Eq. 1). The current comparison of the CV plots 1 and 2 in Fig. 6a suggests that desorption/adsorption of CAQ was slightly faster than that of CA under slow potential scan.

As expected, the CVs of both species present an anodic peak P_a and the corresponding cathodic peak P_c. The positive current values represent the decrease of the amount of CA or the increase of the amount of CAQ in the thin-layer solution, while the negative means the reverse. Further, the CVs for CA and CAQ in the deposited states can be obtained by subtracting the contributions of the species in free solution (Fig. 6a) from the measured CV (Fig. 5a), as shown in Fig. 6b. Therefore, the deposited amount (Γ, in moles per square centimeter) of CA can be evaluated from the CV curve (1) in Fig. 6b and using the equation $\Gamma = A_{pa}/nFA_s v$, where A_{pa} is the area of the anodic peak P_a after background correction, A_s is the electrode area (0.8 cm^2), and the other symbols have their usual meanings. The result obtained for

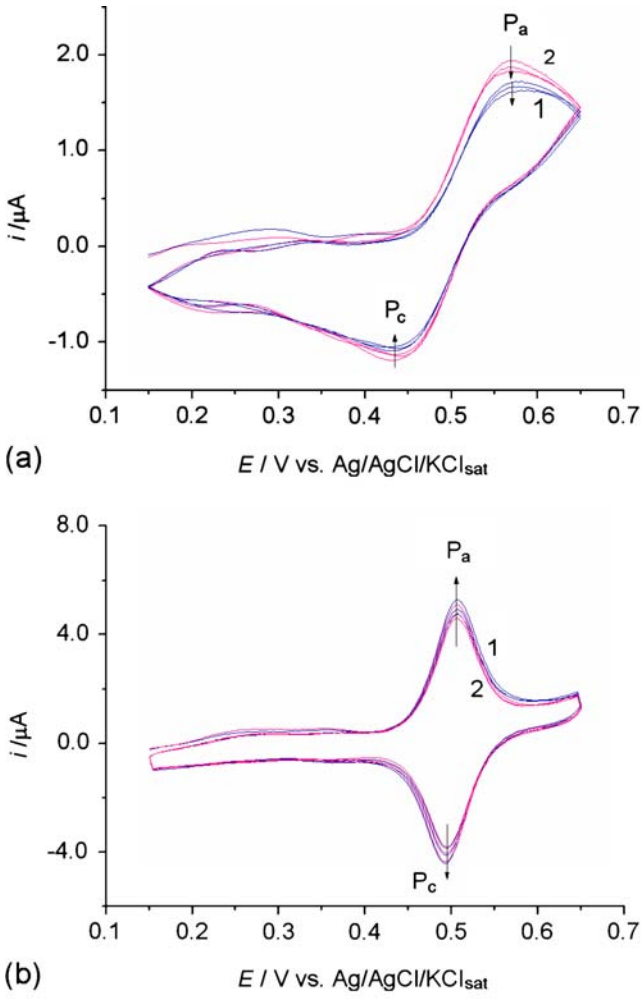

Fig. 6 CVs derived from the DCVAs in Fig. 5c, for CA (*1*) and CA quinone (*2*) in free solution (**a**) or in deposited state (**b**)

the first cycle is about 8.4×10^{-10} mol cm^{-2} (see Table 1), which is very close to the surface coverage of CA on GC electrode measured by Zare and Habibirad in a CA-free solution after modification [2]. The deposited amount increased with the cycle number, n_{cyc}, since the peak currents shown in Fig. 6b increased with n_{cyc}. In the work of Zare and Habibirad, eight cycles of potential were selected as the optimum number for the electrode modification [2]. On the other hand, the CV peak currents of the species in free solution shown in Fig. 6a decreased with n_{cyc}; thus, the slight increase of the measured total currents with n_{cyc} (see Fig. 5a) should be due to the increasing deposited amount of CA on the electrode surface. Peak–current comparison of Fig. 6a

Table 1 Effect of scan rate on the deposited amount of CA on carbon-paste electrode

v/mV s^{-1}	2	5	20
$A_{pa}(CA_{dep})/10^{-7}$ A V	2.6	5.2	16
$\Gamma/10^{-10}$ mol cm^{-2}	8.4	6.7	5.2

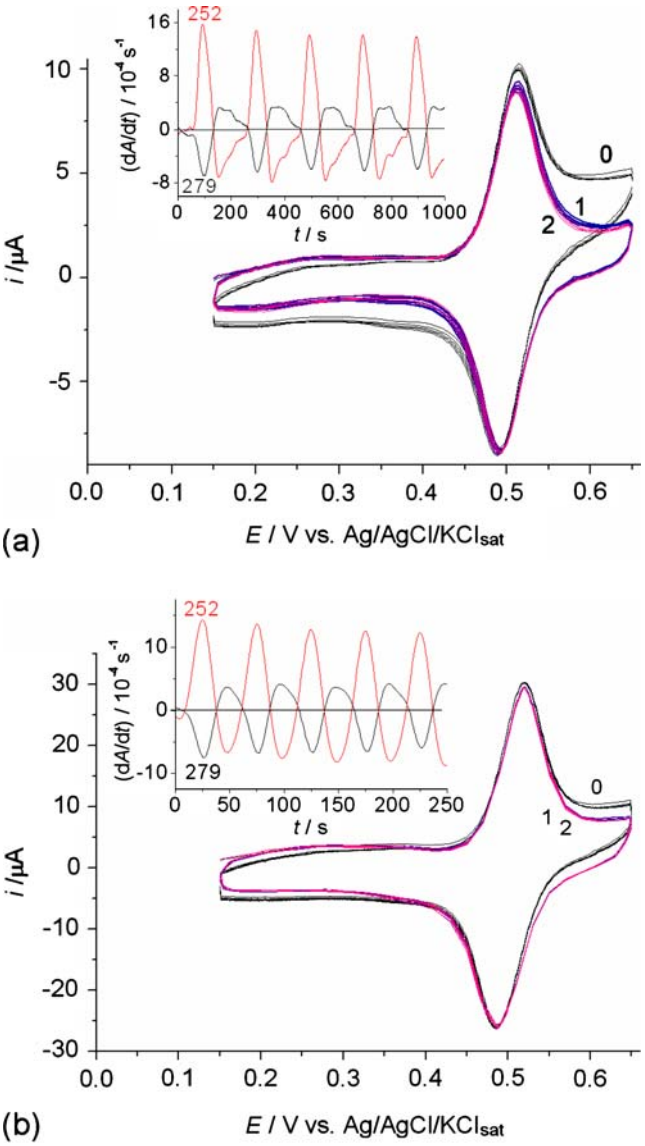

Fig. 7 CVs of 0.1 mM CA (pH=1.8) recorded experimentally (*0*), derived from the DCVAs for CA (*1*) and CA quinone (*2*) in deposited state. Curves *1* and *2* nearly coincide with each other. Scan rates, **a** 5 mV s^{-1}, **b** 20 mV s^{-1}; cycle number, 5. *Insets*: time-derivative chronoabsorptomograms obtained at wavelengths 279 and 252 nm

and b shows that the contributions of the species in deposited state to the total redox currents were more than three times as great as those from the species in free solution, under the present experimental conditions.

Effect of scan rate on the deposition of CA

Effect of scan rate on the deposition of CA was investigated by the CVA measurements. Figure 7a and b shows the results derived from the data recorded at two faster scan rates 5 and 20 mV s^{-1}, respectively. The two CVs derived for CA and CAQ in deposited state nearly coincided with each other, suggesting that the surface coverage of electrode almost

remained unchanged during the redox transition. The voltammetric peaks in all three CVs (one measured and two derived) showed little rise in height with the increasing cycle number (nearly no change at 20 mV s^{-1}), indicating that the redox process was repeatable and stable with the repeating scans. With the increase of scan rate, the peak currents in the CVs of the deposited species (curves 1 and 2) approached the total peak currents in the measured CVs (curve 0), that is, the contribution of the species in free solution to the total current decreased further with the increase of scan rate, as generally expected. Table 1 presents the deposited amounts of CA, which decreased with the increasing scan rate.

Conclusions

The first voltammetric couple of (+)-CA on carbon-paste electrode was quasireversible, pH-dependent, and adsorption-controlled, leading to an electroactive and stable CA film deposited on the electrode surface in pH=1.8 acidic solution. The combination of cyclic voltabsorptometry with voltammetry produced four CVs, which were attributed to CA and its oxidized state, in free solution or in deposited state, respectively. The surface coverage of electrode can be evaluated from the CV obtained for the deposited CA, which decreased with the increasing scan rate. The deposited CA slightly increased in amount with the increasing cycle number and made a major contribution to the total voltammetric current, especially at higher scan rates. Using CA electrodeposited on carbon-paste electrode as a model system, this work demonstrated the usefulness of the time-derivative cyclic voltabsorptometry for voltammetric characterization of the deposited films in the case when not only the deposited species but also the same ones in free solution participated in redox processes.

Acknowledgements The authors gratefully acknowledge financial support from the National Natural Science Foundation of China (No. 20776033) and the Special Foundation for PhD Program in HFUT (No. 2007GDBJ018).

References

1. Salimi A, Abdi K, Khayatian G-R (2004) Mikrochim Acta 144:161 DOI 10.1007/s00604-003-0048-7
2. Zare HR, Habibirad AM (2006) J Solid State Electrochem 10:348 DOI 10.1007/s10008-005-0683-5
3. He J-B, Jin G-P, Chen Q-Z, Wang Y (2007) Anal Chim Acta 585:337 DOI 10.1016/j.aca.2007.01.004
4. Andrade GFS, Temperini MLA (2007) J Solid State Electrochem 11:1497 DOI 10.1007/s10008-007-0318-0
5. Kulesza PJ, Zamponi S, Malik MA, Miecznikowski K, Berrettoni M, Marassi R (1997) J Solid State Electrochem 1:88 DOI 10.1007/s100080050027
6. Huang L-M, Wen T-C, Gopalan A (2006) Electrochim Acta 51:3469 DOI 10.1016/j.electacta.2005.09.049
7. Agrisuelas J, Giménez-Romero D, García-Jareño JJ, Vicente F (2006) Electrochem Commun 8:549 DOI 10.1016/j.elecom.2006.01.022
8. Alpatova NM, Ovsyannikova EV, Topolev VV, Grosheva MY (2004) Russ J Electrochem 40:229 DOI 10.1023/B:RUEL.0000019658.92222.20
9. Astuti Y, Topoglidis E, Gilardi G, Durrant JR (2004) Bioelectrochemistry 63:55 DOI 10.1016/j.bioelechem.2003.09.014
10. Ascone I, Zamponi S, Cognigni A, Marmocchi F, Marassi R (2005) Electrochim Acta 50:2437 DOI 10.1016/j.electacta.2004.10.066
11. Cren-Olive C, Hapiot P, Pinson J, Rolando C (2003) J Am Chem Soc 124:14027 DOI 10.1021/ja0262434
12. Mukai K, Nagai S, Ohara K (2005) Free Radic Biol Med 39:752 DOI 10.1016/j.freeradbiomed.2005.04.027
13. Janeiro P, Brett AMO (2004) Anal Chim Acta 518:109 DOI 10.1016/j.aca.2004.05.038
14. Castaignede V, Durliat H, Comtat M (2003) Anal Lett 36:1707 DOI 10.1081/AL-120023610
15. Vestergaard Md, Kerman K, Tamiya E (2005) Anal Chim Acta 538:273 DOI 10.1016/j.aca.2005.01.067
16. Martinez S, Valek L, Petrović Ž, Metikoš-Huković M, Piljac J (2005) J Electroanal Chem 584:92 DOI 10.1016/j.jelechem.2005.07.015
17. Kilmartin PA, Hsu CF (2003) Food Chem 82:501 DOI 10.1016/S0308-8146(03)00066-9
18. Kilmartin PA, Zou H, Waterhouse AL (2001) J Agric Food Chem 49:1957 DOI 10.1021/jf001044u
19. Guyot S, Vercauterent J, Cheynier V (1996) Phytochemistry 42:1279 DOI 10.1016/0031-9422(96)00127-6
20. Golabi SM, Nematollahi D (1997) J Electroanal Chem 420:127 DOI 10.1016/S0022-0728(96)04804-8
21. He J-B, Wang Y, Deng N, Lin X-Q (2007) Bioelectrochemistry 71:157 DOI 10.1016/j.bioelechem.2007.03.003
22. Brett CMA, Brett AMO (1993) Electrochemistry: principles, methods and applications. Oxford University Press, Oxford
23. Mochizuki M, Yamazaki S-I, Kano K, Ikeda T (2002) Biochim Biophys Acta 1569:35